Chemistry of Inorganic Materials 1 (2023) 100005

Contents lists available at ScienceDirect

Chemistry of Inorganic Materials

journal homepage: www.elsevier.com/locate/cinorg

Rational design of hierarchically porous sulfonic acid and silica hybrids with highly active sites for efficient catalytic biodiesel synthesis

Mehulkumar L. Savaliya [a,b], Ravi S. Tank [a], Bharatkumar Z. Dholakiya [b,*]

[a] Faculty of Science, Department of Industrial Chemistry, Atmiya University, Yogidham Gurukul, Kalawad road, Rajkot, 360005, Gujarat, India
[b] Department of Chemistry, Sardar Vallabhbhai National Institute of Technology (SVNIT), Ichchhanath, Surat, 395007, Gujarat, India

ARTICLE INFO

Keywords:
Castor oil
Fatty acid methyl ester
Heterogeneous catalyst
Transesterification
p-toluene sulfonic acid
Calorific value

ABSTRACT

Catalysis is the vertebra of most of commercial processes, which utilizes chemical reactions to transform reagents into value added chemicals. Biodiesel synthesis from animal fats and edible vegetable oils via transesterification over homogeneous catalysts is recently taken into account of untenable by the emerging biofuel industries, particularly by virtue of food *vs.* fuel counteraction, economic and environmental challenges blended with the feedstocks as well as catalytic systems, respectively. Therefore, present efforts concern with the preparation of a novel PTSA-Si catalyst and its relevance for biodiesel synthesis from non-food castor oil. It has been manifested from the experimental outcomes, the most relevant reaction parameters are, 5% PTSA-Si *(w/w)*, 65 °C reaction temperature, 1:11 O:M molar ratio and 10 h reaction time for 98.56% biodiesel yield. The PTSA-Si was appropriately analyzed using FT-IR, SEM, XRD, BET, TGA-DTA and TPD-NH_3 analysis. Since, castor oil and castor biodiesel were analyzed using FT-IR, ^1H &^{13}C NMR analysis. Besides, biodiesel physico-chemical properties were predicted and associated with ASTM fuel standards.

1. Introduction

The wind, solar and biomass energy are potential substitute in the direction of petroleum based fuels and are excellent commercial sources of renewable energy [1]. The insistence of biofuels as a green fuel is accelerated advancement in the last decennium with a view to reduce our obsession on petroleum based fuels as a leading source of transportation fuel as per the Kyoto protocol on emission control of greenhouse gases [2]. Biofuels are compounds originated from biomass that could directly be a substitute for, or be used as mixture with conventional transportation fuels [3]. The biodiesel is a class of biofuel that could be prepared from variety of feedstocks, assorted into three main groups (i) vegetable oils, (ii) animal fats and (iii) waste frying oils [4]. A fourth group of developing attention are the algal oils offering great oil productiveness. However, the utilization of algal oil as an alternative is still very finite due to high attributed expenses [5]. Presently, cooking oils are being used in more than 95% of the global biodiesel preparation [6]. The major sense behind utilization of cooking oil for biodiesel preparation is that they are easily accessible from massive agricultural formulation enterprises. Nonetheless, this is not a favourable direction due to the significant percussions on food chain inviting to the so known as food *vs.* fuel conflict [7]. To date, considerable non food oils have also been examined as raw materials for biodiesel preparation along with seed oils of jatropha curcas, calo-phyllum inophyllum, tobacco, rubber, mahua, karanja, castor and schleichera oleosa [8]. Among all the oil crops, the castor oil has the considerable oil yield capacity. It offers the higher yield of seeds and oil compositions in its seeds. The major composition of ricinoleic acid is responsible for the higher viscosity and density of castor oil. It has a potential to get dissolved in alcohol, which favours the transesterification reaction. The main sense behind selection of castor oil as feedstocks for biodiesel preparation in present study is its higher production in India, lower economical cost and relevant fuel properties [9]. The physicochemical properties of castor oil are listed in Table 1.

An interest of biodiesel as a green option to conventional fuel comprise its engine affinity and higher engine wear, high transportability, easily availability, eco-friendliness, better combustion performance, better energy generation, low sulfur and aromatic compositions, leading cetane index and greater biodegradability [12]. The combustion of biodiesel offers more than 90% decrease in the total unspent hydrocarbons and a 75–90% weakens cyclic aromatic hydrocarbons emission related to the utilization of petroleum based fuels. Biodiesel also demonstrates a noteworthy shrinkage in particulates matters as well as CO with respect to fossil fuel [13]. The biodiesel is being prepared by using homogeneous alkali and acidic catalysts like,

* Corresponding author.
E-mail addresses: mehulkumar.savaliya@atmiyauni.ac.in (M.L. Savaliya), ravi.tank@atmiyauni.ac.in (R.S. Tank), bharat281173@gmail.com (B.Z. Dholakiya).

https://doi.org/10.1016/j.cinorg.2023.100005
Received 6 December 2022; Received in revised form 26 April 2023; Accepted 1 May 2023
Available online xxxx

Table 1
Physicochemical properties of castor oil [10,11].

Sr. No.	Properties	Value
1.	FFA (%)	0.264
2.	Density (kg/m^3)	962.8
3.	Fire point (°C)	335
4.	Flash point (°C)	298
5.	Cloud point (°C)	15.8
6.	Calorific value (kJ/kg)	35684.5
7.	Kinematic viscosity (mm^2/s)	43.1
8.	Specific gravity	0.962
9.	Cetane number	40
10.	Iodine value (gI_2/100 g)	100

KOH, NaOH, H_2SO_4, HCl and HNO_3 [14]. However, the biodiesel preparation using heterogeneous catalysts contributes a potential substitutive way for their economical production [15]. Solid acids offer several intrinsic advantages over liquid counterparts such as, easy separation, simple post treatment, less waste emission and higher thermal stability [16,17]. Many solid acids have been developed to compensate the conventional liquid acids catalysts. However, most of the solid acid catalysts are less stable, less active and more expensive than the liquid acid catalysts [18]. Solid acid catalysts offer economic and process benefits, especially for low cost feedstocks with high FFA content, enabling single step esterification and transesterification of bio oils [19]. A wide range of solid acids including heteropolyacids [20–22], sulfonated metal oxides [23,24], carbons [25], and zeolites [26] have been employed for biodiesel preparation, nevertheless, novel materials with tailored solvothermal stability and recyclability are still sought. Mesoporous solid acid catalysts are attractive in heterogeneous catalysis with a view to their tunable pore architectures, high surface areas, associated improved mass-transport and potential to generate highly dispersed and active sites [27]. There are several reports available for the single step biodiesel preparation from waste oils using solid acids, including carbon based solid acid [28], active clay [29], Zr-SBA-15 [30] and sulfated tin oxide [31]. The waste oils contain FFAs and triglycerides; both of them form biodiesel. Several benefits of biodiesel in association with petroleum based diesel are that it is environment friendly and safer to use, as it is being prepared from sustainable resources and contains little amounts of sulfur. Even though, the cold flow assets, NOx discharge and higher production expenses are major countenance that have to be defeated [32].

With the above considerations, a novel heterogeneous acid catalyst of silica fused *p*-toluene sulfonic acid was freshly prepared by chemical and physical modification of toluene and silica gel respectively. The synthesized PTSA-Si was examined for single step biodiesel production via transesterification of non food castor oil. It has been concluded from the transesterification results of non food castor oil, the excellent experimental parameters for the maximum biodiesel yield (98.56%) are, 5% PTSA-Si *(w/w)*, 65 °C reaction temperature, 1:11 O:M molar ratio and 10 h reaction span. The synthesized PTSA-Si has been assessed for repeatability study and commenced to be four time successfully reusable without loss of their catalytic performance. The castor oil biodiesel has also been examined for their physico-chemical properties estimation. It has been observed from the study that all physico-chemical properties are found to be within limits prescribed by ASTM standards.

2. Materials and method

2.1. Materials

The methanol (≥99.0%, EMPLURA), silica gel (96.1%, 60–120 mesh), toluene (≥99.0%, EMPLURA), sodium sulphate (99.0%, FINAR), sulfuric acid (99.9%, RANKEM), methylene dichloride (99.8%, FINAR) and *n*-hexane (99.9%, FINAR) were furnished by Aashka Scientific Co., Surat, Gujarat. The castor oil was purchased from local oil trader (Malhar trading), Surat, Gujarat, India. All reagent utilized in the present study were of analytical grade and employed without additional purification.

2.2. Instrumental techniques

The FT-IR spectrum PTSA-Si was executed on a FT-IR spectrometer (Shimadzu). However, the FT-IR analysis of castor oil and castor biodiesel were carried out on another FT-IR spectrometer (PerkinElmer). The ^{1}H NMR and ^{13}C NMR analyses were done on a FT-NMR spectrometer (Bruker 400 MHz NMR). The castor biodiesel (%) yield was calculated on GC analysis (YL 6500 GC, SUPELCO C_8– C_{24} FAME mixture). The wide angle X-ray diffraction pattern was recorded on XRD (Rigaku). The specific surface area of PTSA-Si was predicted on a porosimeter (2020, ASAP). The thermal strength of PTSA-Si was identified by TGA (PerkinElmer). The superficial morphologies of PTSA-Si were recognized by SEM (S3400 N, Hitachi). The total bronsted acid sites in the PTSA-Si were predicted by TPD-NH_3 analysis (Chemisorb 2750).

2.3. Experimental

2.3.1. Synthesis of PTSA-Si hybrids

The PTSA-Si has been prepared by diminutive modification of the reported method [33]. A 100 mL of toluene and 20 mL of concentratedsulfuric acid were transferred in a 250 mL glass reactor (FBF, adapted with a dean stark assembly). The flask was heated with reflux at 160 °C for 6 h. The water droplets began to produce at the same time as a starting of the sulfonation reaction. The quantity of water collected in the dean stark collector was measured at regular interval of times. On the completion of 5 h of sulfonation, a 12.1 mL of water was measured and the sulfonation was extended as far as no further water was produced. On the completion of sulfonation, the heating was interrupted and reaction mass was acquiesced to cool at ambient temperature. The crystallization of *p*-toluene sulfonic acid (PTSA) has been carried out through addition of 30 mL of distilled water. The PTSA has been isolated from the reaction mass and washed with again 10 mL of water. The PTSA has been purified by dissolving in small amount of hot water containing activated charcoal. Finally, the PTSA has been recovered from the aqueous slurry and cooled with ice. A treatment of gaseous HCl to this supper cooled solution leads to the precipitation of white crystals of PTSA (40.18 g). Then after, an equimolar quantity of silica gel was mixed to these white crystals and mechanically stirred at room temperature for 1 h to support PTSA-Si via induction of intermutual hydrogen bonding [34]. Ultimately, a 53.25 g freshly dried light gray fine powder of PTSA-Si was achieved. The reaction strategy for production of PTSA-Si is embossed in Fig. 1.

2.3.2. Catalytic performance test

The transesterification of castor oil was functioned out in 250 mL flat bottom flask, which was adapted with reflux condenser, magnetic stirrer and heating plate system. The required amounts of castor oil, % PTSA-Si (*w/w*) and methanol were calculated stoichiometrically. The desired amount of castor oil was added to flat bottom flask followed by charging of PSTA-Si-methanol mixture. The reflux temperature (65 °C) was maintained and reaction assembly were left uninterrupted for required time period. After the desired length of reaction time, the reaction mixture was carefully shifted to the partition funnel for the partition of the product and by product. The separating funnel was again left uninterrupted till the complete separation of biodiesel and glycerol layers as depicted in Fig. S1. The glycerol collected at the bottom was separated first. The hot distilled water and anhydrous sodium sulphate were used for the refining of biodiesel layer. Consciously to investigate the significance of reaction parameters on the (%) yield of transesterification products, the reactions were carried out by changing catalyst concentration (1, 2, 3, 4, 5 and 6% *w/w*), O:M molar ratio (1:9, 1:10, 1:11 and 1:12) and reaction time (6, 7, 8, 9 and 10 h) at reflux temperature (65 °C). All experiments have been executed in triplicates with a view to find deviations in the biodiesel yield (%) after each successful experiment.

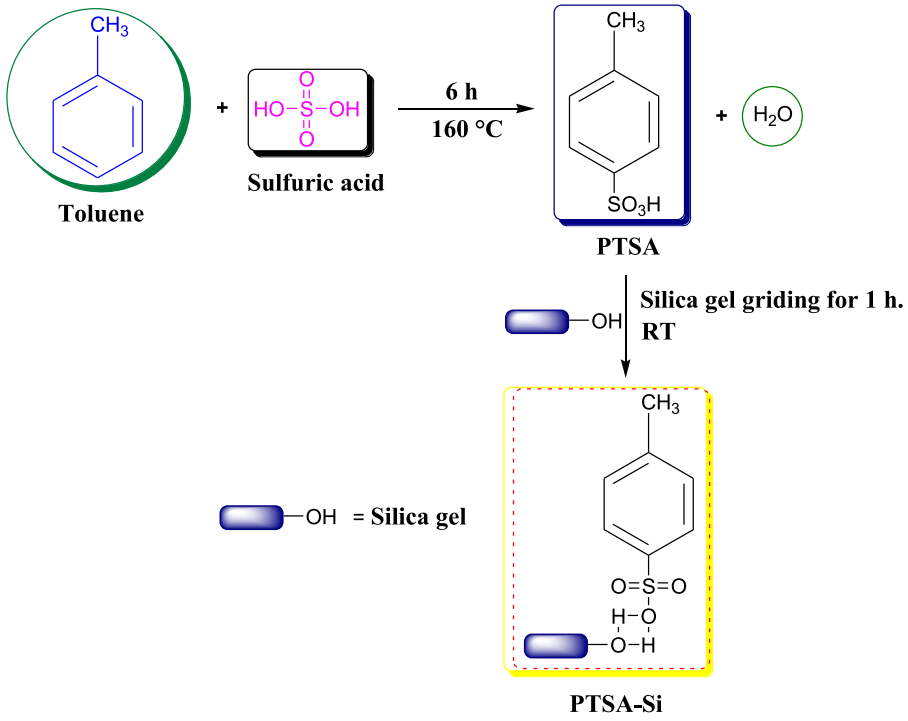

Fig. 1. Reaction scheme for the preparation of PTSA-Si catalyst.

The scheme for the transesterification of castor oil has been demonstrated in Fig. 2.

2.3.3. Biodiesel (%) yield estimation

The castor biodiesel (%) yields and their fatty acid methyl esters distribution were measured though GC investigation. The C_8– C_{24} composition biodiesel mixture (SUPELCO) was involved as a measure for qualitative and quantitative persistence of biodiesel composition on GC (specification: (30 m × 0.320 mm × 0.25 μm, FID, column: Agilent DB-Wax-123-7032)). The peak areas have been accounted for the projection of fatty acid methyl esters composition of each castor biodiesel sample after fatty acid methyl esters of the castor biodiesel samples were identified. The conversion and (%) biodiesel yield were calculated by following formula (i) and (ii) [35].

$$C = \frac{\sum A - A_{IS}}{A_{IS}} \times \frac{C_{IS} \times V_{IS}}{m} \times 100 \quad (1)$$

Where, C stand for the fatty acid methyl ester content, $\sum$ A represent the total peaks area, A_{IS} refers to the methyl heptadecanoate (internal standard) peak area, C_{IS} and V_{IS} stands for the concentration (mg/mL) and volume of internal standard (mL) respectively. The m stands for the quantity of the castor biodiesel (mg).

$$\text{Castor biodiesel yield } (\%) = \frac{M_{Biodiesel} \times C}{M_{Oil}} \times 100 \quad (2)$$

Where $M_{Biodiesel}$ represent the quantity of refined fatty acid methyl esters obtained, M_{Oil} stand for the quantity of castor oil selected and C stand for the fatty acid methyl ester content estimated as mentioned through equation (i). It has been found from the gas chromatogram of castor biodiesel, the prepared biodiesel is offers several methylated fatty acids like methyl ricinoleate, methyl oleate, methyl linoleate and methyl stearate. The GC-FID chromatogram of castor biodiesel is mentioned in Fig. S2.

2.3.4. Mechanism of transesterification of castor oil over PTSA-Si

It has been already reported the transesterification of triglycerides (oil) are being catalyzed by either acidic or alkaline catalysts. It involves three successive reversible reactions. It has been observed that in the transesterification reaction chain, the triglycerides is transformed stepwise to diacylglycerol, monoacylglycerol and followed by glycerine, which is associated with the production of 1 mol of biodiesel at each stage [20]. The mechanism of castor oil transesterification also follows the same sequence. These steps composed of (i) Protonation (H^+) of one of the carbonyl group of castor oil through the PTSA-Si (ii) Nucleophilic incursion of the methanol pointing to the carbonyl group that yield a tetrahedral transitional product and (iii) Proton displacement (H^+) and

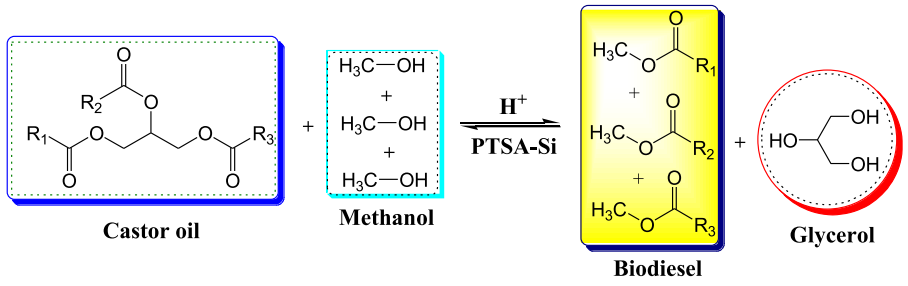

Fig. 2. Reaction scheme for the transesterification of castor oil to biodiesel.

disconnection of the tetrahedral intermediate yields biodiesel and diacylglycerol. The displaced proton repeatedly consumed through the leading PTSA-Si with a view to reproduce it for the next repetitive use. This consolidated continuity will repeat by two times till thorough synthesis of mixture of biodiesel and glycerol. The mechanism scheme for the transesterification of castor oil is given in Fig. 3.

3. Results and discussion

Generally, the transesterification of oil demands a suitable catalyst with a view to obtain desired production rates. The constitution of the catalyst is remains essential since it regulate the configurations restrictions that the raw material must contain. Besides, the reaction parameters and post isolation steps are pre-planned by the attributes of the catalyst employed [36]. Generally, majority of oils are being transformed into biodiesel using alkali catalyzed transesterification method. But there are several uncommon cases wherein direct transesterification cannot be carried out. Such cases appear in raw vegetable oils like olive, jatropha, castor and cotton seed oil, etc. Such raw vegetable oils possess high free fatty acids (FFAs) contents in their oil compositions, as it forms soap on base catalyzed transesterification [10]. Therefore, it is a demand of time to develop an efficient heterogeneous acid catalyst to overcome such problems. Because, the heterogeneous acid catalysts can concurrently conducts transesterification of TGs and esterification of FFAs to biodiesel. Hence, it is not required to isolate free fatty acids from the triglycerides [36]. With the above considerations, in the present study, the biodiesel synthesis has been carried out by transesterification of non food castor oil over PTSA-Si as a solid acid catalyst. In order to optimize the process

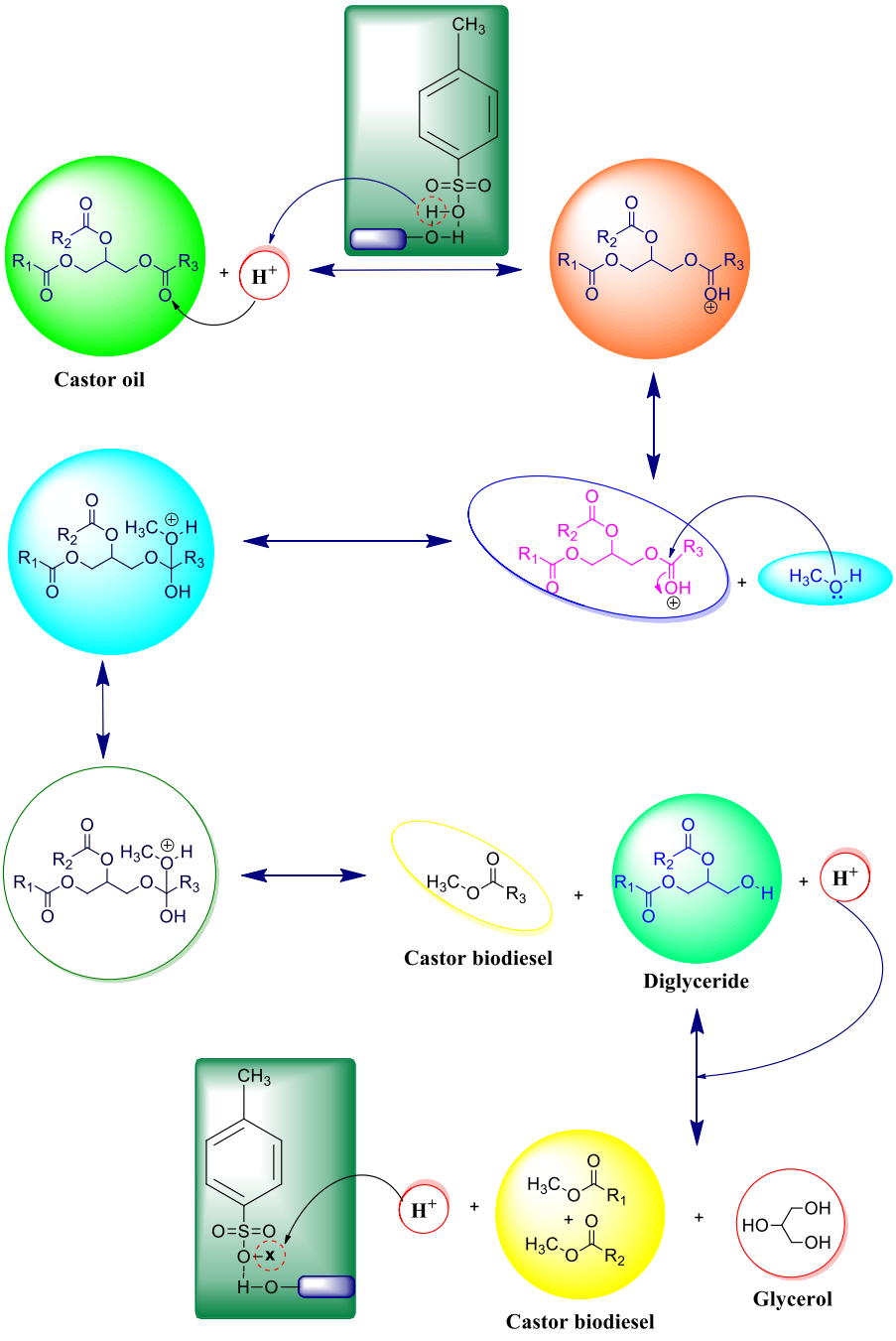

Fig. 3. Proposed reaction mechanism for the transesterification of castor oil to biodiesel.

parameters, the biodiesel reactions were examined by varying catalyst concentration (1, 2, 3, 4, 5 and 6% *w/w*), O:M molar ratio (1:9, 1:10, 1:11 and 1:12) and reaction time (6, 7, 8, 9 and 10 h) at reflux temperature (65 °C). All the experiments were functioned at viscerous pressure till an attainment of the maximum conversions. The results of castor biodiesel yields (%) with distinctive reaction parameters have been tabularized in Table 2.

3.1. Influence of oil to methanol molar ratio

In pursuance to look into the cause of oil to methanol (O:M) molar ratio on biodiesel (%) yields, all reactions were executed out at diverse O:M molar ratio (1:9, 1:10, 1:11 and 1:12). In connection with Tables 2 and it has been confirmed that, the biodiesel yield (%) is precisely influence by diversifying methanol to oil (M:O) molar ratio. The biodiesel (%) yield is gradually increased with the increasing M:O molar ratio. With 1:9, 1:10, 1:11 and 1:12 O:M molar ratio, the maximum biodiesel (%) yields were found to be 80.23%, 88.12%, 98.56% and 94.23% respectively. The optimal biodiesel (%) yield (98.56%) was found with 1:11 O:M molar ratio. The backward reaction (alcoholysis of glycerol and biodiesel) directly enhances upon keeping O:M molar ratio down from 1:11. Accordingly, the reversible nature of the transesterification is the responsible factor for the decrement in (%) yield of biodiesel at O:M molar ratio below 1:11. It has also been perceived that the reduction in the biodiesel (%) yield above 1:11 O:M molar ratio and this may in conjunction to the polar apparent of PTSA-Si and methyl alcohol. Wherefore, it constantly raises the polarity of the transesterification, on increasing of M:O molar ratio. In advance of, the reaction mechanism of transesterification evidently acclaimed that, first oil must react with catalyst. Though, as the quantity of alcohol increases, the reaction mass is also starts to increase its polarity. Therefore, contrary to oil aspect, the PTSA-Si constantly displaced to the alcohol aspect. Wherefore, the connections of PTSA-Si in the direction of methanol phase become absolutely energetic than connections of PTSA-Si in the direction of oil phase. Consequently, the shrinkage in the biodiesel (%) yield was noticed above 1:11 O:M molar ratio. The bar graph indicating an effect of O:M molar ratio approaching biodiesel (%) yield is manifested in Fig. 4.

Table 2
Results of castor biodiesel yield (%) with peculiar reaction parameters at 65 °C.

Sr. No.	O:M molar ratio	Reaction time (h)	% (*w/w*) PTSA-Si	Biodiesel Yield[a] (%)
1.	1:9	6	5%	46.51 ± 0.93
2.	1:9	7	5%	59.36 ± 1.31
3.	1:9	8	5%	65.78 ± 0.70
4.	1:9	9	5%	72.32 ± 0.96
5.	1:9	10	5%	80.23 ± 0.91
6.	1:10	6	5%	58.98 ± 0.96
7.	1:10	7	5%	72.65 ± 0.89
8.	1:10	8	5%	79.25 ± 1.32
9.	1:10	9	5%	83.65 ± 0.78
10.	1:10	10	5%	88.12 ± 0.81
11.	1:11	6	5%	68.54 ± 0.91
12.	1:11	7	5%	80.29 ± 1.28
13.	1:11	8	5%	88.65 ± 1.21
14.	1:11	9	5%	91.32 ± 0.98
15.	1:11	10	5%	98.56 ± 0.99
16.	1:12	6	5%	66.32 ± 1.11
17.	1:12	7	5%	77.54 ± 0.78
18.	1:12	8	5%	86.32 ± 1.09
19.	1:12	9	5%	90.32 ± 1.16
20.	1:12	10	5%	94.23 ± 0.93
21.	1:11	10	1%	22.34 ± 1.31
22.	1:11	10	2%	38.35 ± 0.70
23.	1:11	10	3%	54.23 ± 1.11
24.	1:11	10	4%	82.56 ± 1.02
25.	1:11	10	6%	98.24 ± 0.98

[a] *(n=3) All experiments have been carried out in triplicates.*

3.2. Influence of reaction time (h)

In pursuance to look into the effect of reaction span (h) in direction of biodiesel (%) yield, all experiments were studied employing diversified span of reaction times (6, 7, 8, 9 and 10 h). In connection with Tables 2 and it has been perceived that the 1:11 O:M molar ratio demonstrates optimum yield of biodiesel (98.56%). Thus, 1:11 O:M molar ratio was preferred as an optimal ratio to examine biodiesel synthesis employing diversified span of reaction times. From the observations, it can be evidenced that, with 6 h, 7 h, 8 h, 9 h and 10 h reaction times, the optimal biodiesel (%) yields observed were 68.54%, 80.29%, 88.65%, 91.32% and 98.56% respectively. alongside 10 h reaction time, it indicates almost complete conversion of castor oil into biodiesel, thus, the reaction time (h) was not studied beyond 10 h span. The bar graph indicating an effect of reaction time (h) approaching biodiesel (%) yield has been manifested in Fig. 5.

3.3. Influence of PTSA-Si quantity (% w/w)

In pursuance to look into the cause of PTSA-Si quantity (% *w/w*) on biodiesel (%) yields, all experiments were executed by shifting PTSA-Si concentration (1, 2, 3, 4, 5 and 6% *w/w*). In connection with Tables 2 and it was realized that, the biodiesel (%) yield increases on increasing the catalyst quantity (% *w/w*). In the case of 1%, 2%, 3%, 4%, 5% and 6% catalyst quantity *(w/w)*, the biodiesel (%) yield were found to be 22.34%, 38.35%, 54.23%, 82.56, 98.56% and 98.24% respectively at optimum O:M molar ratio. The PTSA-Si quantity above 5% (*w/w*) doesn't symbolize any noticeable improvement in the biodiesel (%) yield rather the (%) yield of biodiesel is slight decreased with 6% catalyst due to increment of the polarity of the reaction on increment of the % catalyst *(w/w)*. Accordingly, it was observed from the reaction outcomes, as catalyst quantity (% *w/w*) increases, the biodiesel (%) yield also increases. It has also been perceived that the slight reduction in the biodiesel (%) yield with 6% catalyst (*w/w*) and this may in conjunction to the polar apparent of PTSA-Si and methyl alcohol. Wherefore, it constantly raises the polarity of the transesterification, on increasing of PTSA-Si concentration. In advance of the reaction mechanism of transesterification evidently acclaimed that, first oil must react with catalyst. Though, as the concentration of catalyst increases, the reaction mass is starts to increase its polarity. Therefore, contrary to oil aspect, the PTSA-Si constantly displaced to the alcohol phase. Wherefore, the connections of PTSA-Si in the direction of methanol phase become absolutely energetic than connections of PTSA-Si in the direction of oil phase. The bar graph indicating an

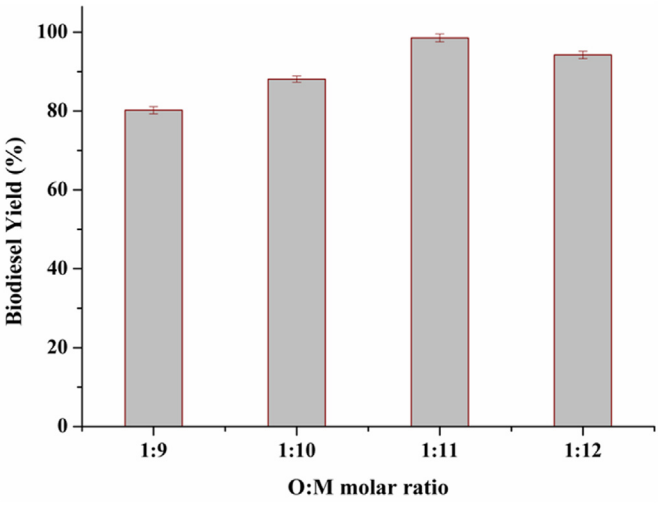

Fig. 4. Impact of oil to methanol molar ratio on the (%) yield of biodiesel (Reaction time: 10 h and PTSA-Si: 5% (*w/w*)).

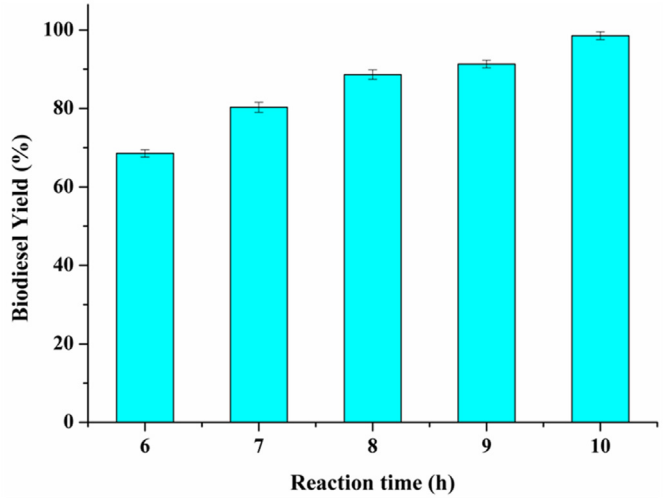

Fig. 5. Impact of reaction time (h) on the (%) yield of biodiesel (O:M molar ratio: 1:12 and PTSA-Si: 5% (*w/w*)).

effect of PTSA-Si quantity (% *w/w*) approaching biodiesel (%) yield is manifested Fig. 6.

3.4. FT-IR analysis of PTSA-Si

The FTIR spectroscopy is a precise technique being used particularly for identifying organic chemicals in a whole range of applications. An absorption pattern of synthesized PTSA-Si catalyst is accustomed by the existence of characteristic bands at 3439.19 cm^{-1}(stretching, intermolecular H- bonding, O–H), 3036.06 cm^{-1} (stretching, C–H), 2918.40 cm^{-1} (stretching, CH_3), 1629.90 cm^{-1} (bending, C═C), 1206.33 cm^{-1} (stretching, C–S), 1143.83 cm^{-1} (stretching, O═S═O (by virtue of –SO_3H group)), 1066.67 cm^{-1} (stretching, S═O), 1016.52 cm^{-1} (stretching, O–Si–O), 815.92 cm^{-1} (*p*-substituted benzene ring) and 692.47 cm^{-1} (bending, C–H) subsequently. The FT-IR graph of PTSA-Si is mentioned in Fig. 7.

3.5. Morphological study of PTSA-Si catalyst

An external morphology and structural orientation of PTSA-Si has been studied by scanning electron microscopic analysis. It has been observed from the SEM micrographs of PTSA-Si catalyst, the PTSA

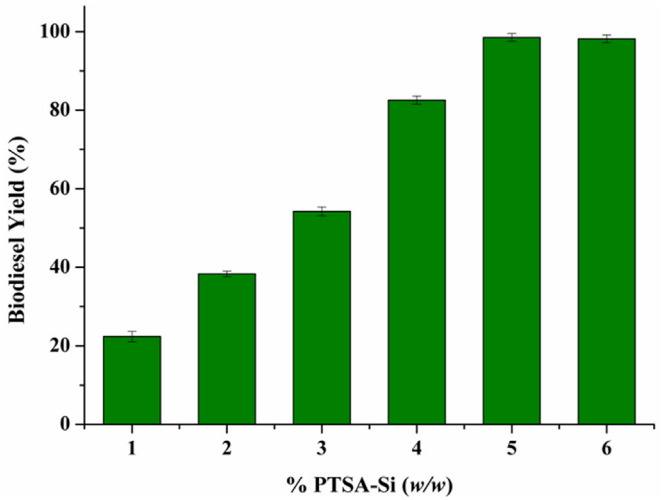

Fig. 6. Impact of % PTSA-Si (*w/w*) on the (%) yield of biodiesel (O:M molar ratio: 1:11 and Reaction time: 10 h).

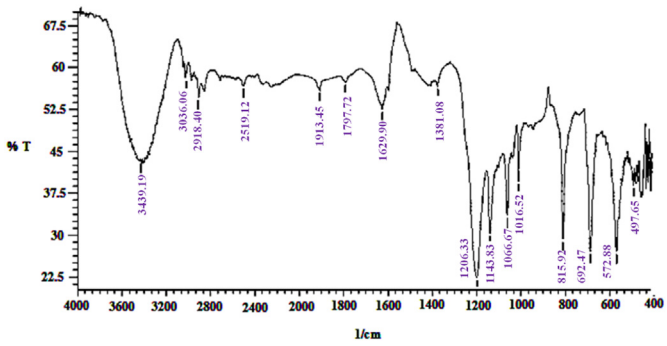

Fig. 7. FT-IR spectrum of PTSA-Si.

particles are found with aggregates of irregular size and shapes after sulfonation with sulfuric acid. Whereas, the silica gel particles are found with finer needles of pentagonal shape. It has been well reported that silica particles are found to have smoother surface. However, on treatment with *p*-toluene sulfonic acid, they are found with rough surface. The average particle size of PTSA-Si has been found in the range of 1.07–1.66 μm. Muthu et al. (2014) have synthesized sulfated zirconia catalyst via solvent free method and evaluated for the biodiesel synthesis using neem oil. From the SEM micrograph of sulfated zirconia, they realized that the particle size of sulfated zirconia is in the range of 20–30 μm and is in an agglomerated form on calcination at 600 °C [37]. The SEM micrographs of PTSA-Si are picturized in Fig. 8.

3.6. The crystalline structure of the PTSA-Si

The texture characteristics of PTSA-Si were analyzed by X-ray diffraction analysis. The X-Ray diffractogram displayed characteristics diffraction pattern showing crystalline nature of PTSA-Si. The diffractogram displayed particular diffraction impression confirming crystalline texture of PTSA-Si. The particular peaks recognized at 2θ = 9.22 (deg.) (face-centered cubic), 2θ = 13.04 (deg.) (body-centered cubic), 2θ = 15.14 (deg.) (face-centered cubic/diamond cubic), 2θ = 16.84 (deg.) (body-centered cubic/simple cubic), 2θ = 18.10 (deg.) (face-centered cubic/simple cubic), 2θ = 22.12 (deg.) (simple cubic), 2θ = 24.08 (deg.) (body-centered cubic), 2θ = 24.62 (deg.) (body-centered cubic), 2θ = 25.60 (deg.) (body-centered cubic/simple cubic), 2θ = 27.16 (deg.) (body-centered cubic), 2θ = 28.12 (deg.) (face-centered cubic) and 2θ = 76.16 (deg.) (face-centered cubic) are associated with the existence of silica gel crystals (JCPDS-29-1129). Although, knife-edged peaks observed at 2θ = 31.74 (deg.), 2θ = 34.02 (deg.), 2θ = 38.42 (deg.), 2θ = 42.92 (deg.), 2θ = 43.72 (deg.), 2θ = 45.80 (deg.) and 2θ = 52.68 (deg.) are peculiarity of *p*-toluene sulfonic acid (JCPDS-39-1699). The wide angle X-Ray diffractogram of PTSA-Si has been demonstrated in Fig. 9.

3.7. Determination of thermal stability

The thermal strength of the PTSA-Si was assured by TGA examination. The weight loss of PTSA-Si was measured as behaviour of raise in temperature or heating rate. The TGA-DTA curve of PTSA-Si displays a natural three stage disintegration diagram. The three steps in disintegration diagram can be predicted by loss of moisture, decomposition of sulfonic acid group (-SO_3H) and total degradation and decomposition of PTSA. The first weight loss (10.68%) is observed in temperature domain of 30–150 °C is due to disintegration of absorbed moisture on catalyst surface. The second weight loss (45.03%) is observed in temperature domain of 150–400 °C is accredited with the disintegration of sulfonic acid groups (-SO_3H) of the toluene. The second derivative of DTA also confirms the disintegration of sulfonic acid groups from the toluene. However, the third weight loss (5.49%) is observed in temperature domain of 400–910 °C is an account for the decomposition of toluene. In

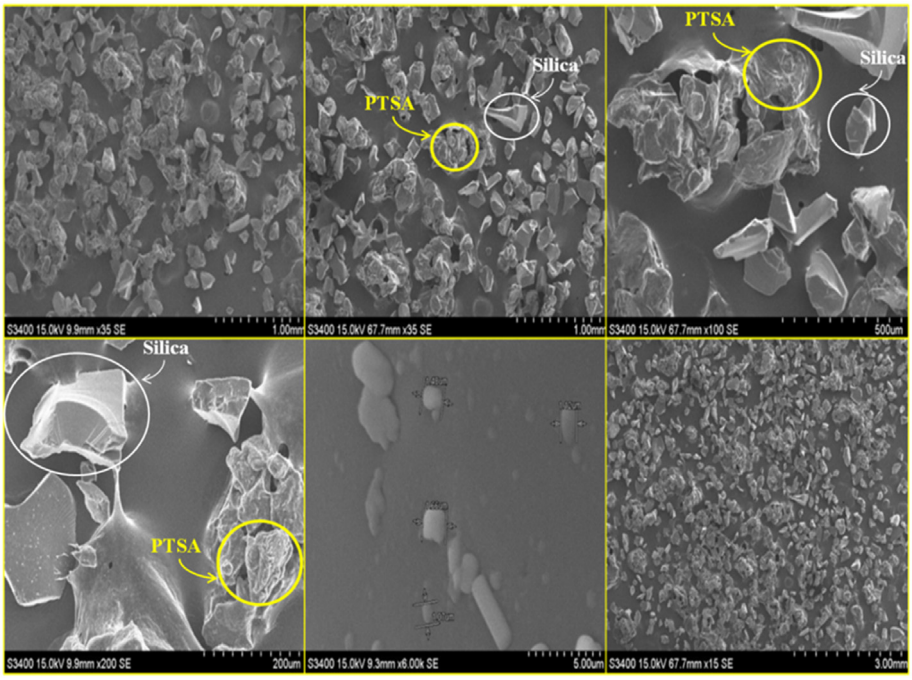

Fig. 8. SEM micrographs of PTSA-Si.

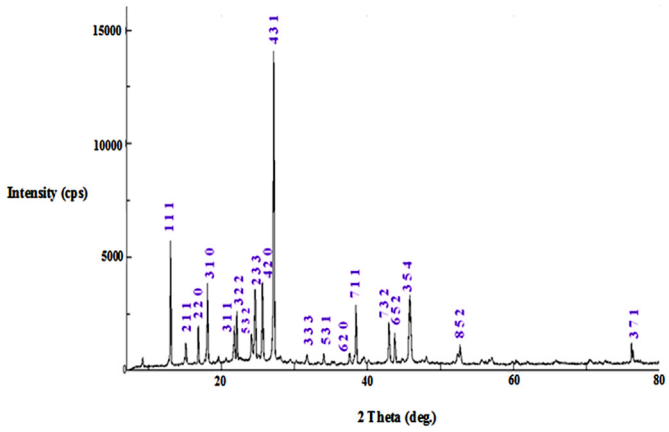

Fig. 9. The wide angel X-Ray diffractogram of PTSA-Si.

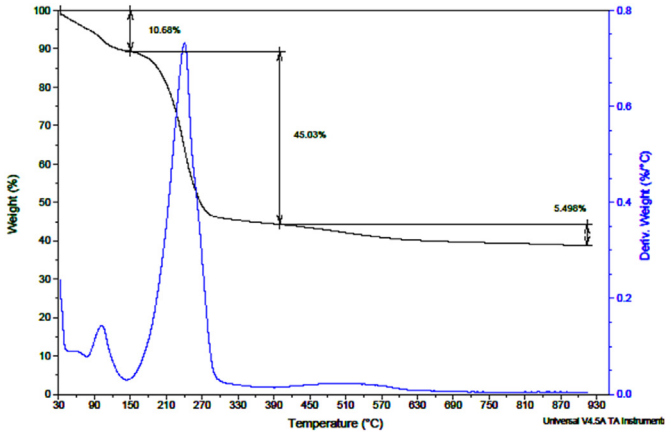

Fig. 10. TGA-DTA profile of PTSA-Si.

the present study all transesterification reactions have been carried out at reflux temperature (65 °C). However, in the TGA curve of PTSA-Si, it was recognized that the first weight loss (10.68%) is observed in temperature scale of 30–150 °C is due to disintegration of absorbed moisture on PTSA-Si surface. Hence, the PTSA-Si offers a better thermal stability at reflux temperature. Ferreira e Santos et al. (2014) have prepared a novel ZrO_2–SiO_2 mixed oxides and evaluated for the thermal stability study. From the TGA thermogram of ZrO_2–SiO_2 mixed oxides, they found that the almost constant decrease of mass in the scale of 100–200 °C, which is due to the decomposition of water, impurities, alkoxides, and unspent solvents. Although, beyond 700 °C temperature, the weight loss is accredited to the dehydroxilation of the catalyst framework [38]. The TGA thermogram of PTSA-Si is depicted in Fig. 10.

3.8. Determination of surface area of PTSA-Si

The specific surface area of PTSA-Si was executed by Brunauer-Emmet-Teller (BET) surface area analysis and the results are tabularized in Table 3.

From the BET isotherm of PTSA-Si, it has been observed that the catalyst offers a specific surface area of 9.61 m^2/g, pore volume of 0.99 cm^3/g and pore size of 2.50 nm. The lower pore volume and pore size itself express that the existence of sulfonic acid (-SO_3H) groups on the porous surface of PTSA-Si catalyst. The hysteresis of PTSA-Si has been found typically of type-IV, which indicates the presence of mesoporous structure of PTSA-Si. This conclusion is also identical with reported literature [39]. Ferreira e Santos *al.* have prepared a novel ZrO2–SiO2 mixed oxides and evaluated for the specific surface area determination. They observed that the catalyst offers a specific surface area of 1742 m^2/g and BET isotherm found of type- IV indicating the presence of mesoporous structure of ZrO2–SiO2 mixed oxides [38]. The BET isotherm of PTSA-Si has been demonstrated in Fig. 11.

Table 3
Results of specific surface area, pore volume and pore size of PTSA-Si.

Sr. No.	Catalyst	Specific surface area (m^2/g)	Pore volume (P/Po) (cm^3/g)	Pore size (nm)
1.	PTSA-Si	9.61	0.99	2.50

3.9. Determination of acidity of PTSA-Si

The total active sites (H^+) in PTSA-Si were measured using TPD-NH_3 analysis and results are tabularized in Table 4.

In connection to the TPD-NH_3 spectrum of PTSA-Si, it was found that the catalyst offers a bronsted acidity of 1.49 mmol/g at 194.8 °C, which confirms the presence of acid/super acid sites on the PTSA-Si surface. Ferreira e Santos et al. have prepared a novel ZrO2–SiO2 mixed oxides and evaluated for the total acidity determination by TPD-NH_3 analysis. From the TPD-NH_3 spectrum of ZrO2–SiO2 mixed oxides, they observed that the catalyst offers an acidity of 476 mmol/g, which affirmed the existence of acid/super acid sites on the sulfonated materials [38]. The TPD-NH_3 spectrum of PTSA-Si is demonstrated in Fig. S3.

3.10. FT-IR analysis of CO

The FT-IR spectrum of castor oil (CO) is accustomed with the presence of characteristics bands at 2926.01 cm^{-1} (CH_3 stretching), 2852.72 cm^{-1} (CH_2 stretching), 2029.11 cm^{-1} (C═C stretching), 1743.65 cm^{-1} (C═O stretching), 1462.04 cm^{-1} (CH bending), 1163.08 cm^{-1} and 1095.57 (C–O stretching) and 725.23 cm^{-1} (CH rocking) respectively. The FT-IR spectrum of CO is illustrated in Fig. S4 (a).

3.11. FT-IR analysis of CB

The FT-IR spectrum of castor biodiesel (CB) is accustomed with the presence of an essential bands at 2926.01 cm^{-1} (CH_3 stretching), 2854.65 cm^{-1} (CH_2 stretching), 2046.47 cm^{-1} (C═C stretching), 1737.86 cm^{-1} (C═O stretching), 1460.11 and 1436.97 cm^{-1} (CH bending), 1195.87, 1172.72 cm^{-1} and 1012.63 cm^{-1} (C–O stretching) and 725.23 cm^{-1} (CH rocking) respectively. The FT-IR spectrum of CB is illustrated in Fig. S4 (b).

3.12. ^{1}H NMR analysis CO

The proton nuclear magnetic resonance (^{1}H NMR) is a spectroscopic technique generally used for structural determination of organic molecules. The structure of castor oil was accustomed by an essential peaks at 5.33–5.40 ppm (unsaturated olefinic –CH═CH- protons), 4.24–4.39 ppm (CH–CH_2 protons), 4.11 ppm (O–CH_2 protons), 3.35–3.39 ppm (-OH protons), 2.50 ppm (α-CH_2 protons), 2.23–2.28 ppm (β-CH_2 protons) and 2.02–2.09 ppm (CH_3 protons) respectively. The ^{1}H NMR spectrum of CO is illustrated in Fig. S5 (a).

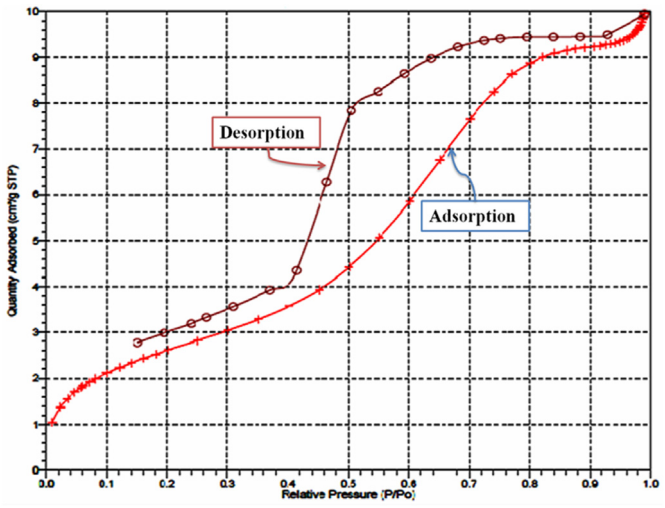

Fig. 11. BET profile of PTSA-Si.

Table 4
Physico-chemical properties of PTSA-Si.

Sr. No.	Catalyst	Temperature at maximum (°C)	Acidity) (mmol/g)	Volume (mL/g STP)
1.	PTSA-Si	194.8	1.49	6.94

3.13. ^{1}H NMR analysis CB

The structure of castor biodiesel was accustomed by the presence of an essential peaks at 7.28 ppm ($CDCl_3$ solvent), 5.28–5.50 ppm (unsaturated olefinic –CH═CH- protons), 4.81–4.84 ppm (CH–CH_2 protons), 3.54–3.60 ppm (CH_3O-methoxy protons), 2.22–2.26 ppm (α-CH_2 protons) and 2.14–2.21 ppm (β-CH_2 protons) respectively. The ^{1}H NMR spectrum of CB is illustrated in Fig. S5 (b).

3.14. ^{13}C NMR analysis of CO

The structure of castor oil was also accustomed by the presence of an essential peaks at 171.98–172.31 ppm (C═O carbons), 126.58–130.26 ppm (olefinic carbons), 69.72 ppm (CH–O carbons), 68.69 ppm (CH_2–O carbons), 61.73 ppm (CH_3 carbon), 36.45–40.08 ppm (DMSO solvent) and 28.39–36.45 ppm (aliphatic carbons) respectively. The ^{13}C NMR spectrum of CO is illustrated in Fig. S6 (a).

3.15. ^{13}C NMR analysis of CB

The structure of castor biodiesel is also accustomed by the presence of an essential peaks at 173.50–176.38 ppm (C═O carbons), 124.27–132.90 ppm (olefinic carbons), 76.82–77.45 ppm ($CDCl_3$-solvent), 63.28–73.62 ppm (CH–O carbons), 51.37 ppm (O–CH_3 carbon) and 27.31–36.78 ppm (aliphatic carbons) respectively. The ^{13}C NMR spectrum of synthesized CB is illustrated in Fig. S6 (b).

3.16. Comparison of catalytic exertion of PTSA-Si

The resemblance of catalytic activity of any catalyst is of significant important in order to ensure the activity of synthesized catalysts with existing literature [36]. Further, it also helps to design an economical viable production process. Table 5 represents the resemblance of catalytic activity of PTSA-Si with outcomes of existing literature for the equivalent class of heterogeneous bronsted acid catalysts examined for biodiesel production through castor oil transesterification.

From Table 5 it was ascertained that PTSA-Si offers noteworthy catalytic execution for the transesterification of castor oil as a means of biodiesel synthesis. In current investigation, the suggested fundamental reaction parameters found for the maximum biodiesel yield (%) are; 65 °C reaction temperature, 1:11 O:M molar ratio, 5% (*w/w*) PTSA-Si and 10 h reaction span, for 98.56% biodiesel conversion. It was also been established from Table 5, the outcomes of the current investigation are conveniently corresponding to the outcomes of existing literature for the identical class of heterogeneous bronsted catalysts, where analogously rigorous reaction conditions were demanded [42,45–48].

3.17. Moisture absorption sensitivity of PTSA-Si

The synthesized PTSA-Si was also evaluated for their moisture absorption sensitivity. Therefore, herein, the prescribed quantity of PTSA-Si was transferred in a glass bottle which kept in stabile wetness at room temperature for certain days with a view to permit the moisture absorption on the PTSA-Si catalyst. The PTSA-Si catalyst was weighed at regular slot of times. The moisture absorption rate (*W*%) of the PTSA-Si catalyst was determined through following formula (iii).

$$W\% = \left[\frac{56\,\Delta m}{18 m_o}\right] \times [100] \quad (3)$$

Table 5
Comparison of catalytic activity of PTSA-Si with reported results (Feedstock: Castor oil).

Sr. No	Catalyst	Reaction Conditions	Biodiesel yield (%)	Ref.	Sr. No	Catalyst	Reaction Conditions
		Reaction Temp. (°C)	Catalyst % (*w/w*)	O:M molar ratio	Reaction time (h)		
1.	PTSA-Si	65	5.0	1:11	10	98.56	Present study
2.	Iron (II) doped zinc oxide nanocatalyst	55	14	1:12	50 min.	91.0	[40]
3.	Sulphonated phenyl silane montmorillonite	60	5.0	1:12	300 min.	89.8	[41]
4.	Super acidic sulfonated modified mica catalyst	60	6.0	1:12	300 min.	90.0	[42]
5.	Supported polyaniline-sulphate	55	4.3	1:29	10	78.0	[43]
6.	Tin (IV) complexes	150	1.0	1:4	4.0	61.0	[44]
7.	Solid supported acidic salt catalyst	70	5.0	1:40	5.0	95.0	[45]
8.	sulfated titania	120	1.0	1:6	1.0	25.0	[46]
9.	Iron nanocatalyst	65	1.0	1:9	150 min.	85.0	[47]
10.	Sulfonated activated-carbons	65	5.0	1:12	60 min	94.0	[48]

Where, Δm belongs to the increased weight and m_0 belongs to the initial weight of the PTSA-Si sample. The impact of moisture exposure time (h) on the moisture absorption rate of PTSA-Si is illustrated in Fig. S7.

From Fig. S7, it was examined that, the moisture absorption profile is continuously increasing alongside increasing in the moisture revelation span (h) up to 90 h. However, beyond 90 h of moisture exposure time (h), the PTSA-Si doesn't display any noteworthy intensification in its weight. It is almost saturated by the atmospheric moisture. The *p*-toluene sulfonic acid (PTSA) surface present a one hydroxyl (-OH) groups in conjunction to one sulfonic (-SO_3H) acid group in their framework. Therefore, due to polar composition of PTSA-Si, it holds a tendency to freely consume the moisture against steady humidity atmosphere.

3.18. Influence of repetitive runs of PTSA-Si on castor biodiesel (%) yield

The production expense of biodiesel itself decides their accessible and large scale commercialization [36]. The catalyst reusability is a considerable feature for the measurement of an economical viability of the production process. Therefore, with an intention to cut down an economical expense of biodiesel production, the PTSA-Si was evaluated for their possible recyclability in the castor oil transesterification. Accordingly, in present work, after each successful cycle, the PTSA-Si was detached out from the reaction batch by means of vacuum separation and mediated with few quantity of methylene dichloride with a view to expel impurities like, unused castor oil, glycerol and unused alcohol. Before the repetitive use, the purified PTSA-Si was putted up in an air dryer at 100 °C for 24 h with a view to remove volatile solvent and regeneration of active centres (H^+) on the toluene surface. It was observed through execution of castor oil transesterification, the PTSA-Si could have a significant potential to recycle four times left out characteristic desertion of catalytic performance. This reusability might be due to the stability of PTSA-Si and the strong attachment of sulfonic acid group (-SO_3H) with toluene. Nonetheless, the minor reduction in the (%) yield of castor biodiesel has been noticed during the repetitive cycles of PTSA-Si. An extraction of active site (H^+) or physicochemical change of PTSA-Si framework at 65 °C temperature could responsible for the deactivation of PTSA-Si. The toluene sustains its structure over the castor oil transesterification without any severe change. The virgin PTSA-Si could displays optimum conversion of castor oil to biodiesel equal to 98.56%. While, it's first, second, third and fourth repetitive run could displays optimum transformations of oil to biodiesel up to 94.25%, 90.26%, 86.28% and 81.20% subsequently. Liu et al. (2008) have synthesized sulfonated ordered mesoporous carbon (OMC-SO_3H) and examined for biodiesel synthesis through esterification of oleic acid. From the reusability study of the OMC-SO_3H catalyst, they concluded that the OMC--SO_3H catalyst can be reusable for four successful times without noticeable loss of catalytic exertion. They also concluded that the reusability is due to the thermal stability of OMC-SO_3H and the strong coupling of sulfonic acid group with carbon [49]. An impact of PTSA-Si runs on the biodiesel (%) yield is exemplified in Fig. 12.

3.19. Assessment of fuel properties of castor biodiesel

The castor oil plant grows in a hot and humid environment; it has a growing season of 4–5 months. The castor oil is a colourless to very pale yellow viscous liquid with moderate or no odour or taste. Castor oil offers a very lower pour and cloud points which make castor biodiesel a good alternative in winter season [50]. The physico-chemical properties of biodiesel can diversify considerably from one raw material to another owing to its somewhat high molecular mass than conventional diesel. The considerable fuel standard systems like ASTM, AOCS, IS, JIS, BS and EU are fruitful for the correlation of the physico-chemical properties of biodiesel produced from diversified oils. The physico-chemical properties are useful for any fuel to determine their engine performance, emission, storage and transportations conditions. The fuel properties of castor biodiesel with contrast to ASTM standards have been tabularized in Table 6.

The cetane number was measured on cetane analyser (AFIDA 2805). The density of castor biodiesel was measured by hydrometer mechanism. The acid and iodine values have been measured by titration methods. The specific gravity of biodiesel has been calculated using specific gravity bottles. Flash and fire points were predicted by closed cup tester (ADITYA-SUNBIM). The refractive index has been measure by refractometer (Anton parr, abbemat 300). The cloud and pour points have been determined on cloud and pour point analyzer (ALANready, CPP 5Gs). The calorific value of castor biodiesel has been determined through oxygen bomb calorimeter (Parr 6400 calorimeter). The kinematic viscosity and viscosity were measured on viscometer (Aditya 01). From Tables 6 and it was recognized that all physico-chemical properties of castor biodiesel are according to the test restrictions, which are established by ASTM standards.

3.20. Industrial aspect of the process

An economical viability is very necessary with a view to explore preparation of biodiesel at commercial spectrum [36,51]. When small-scale manufacturers embark on survey of the finances of biodiesel production, they frequently discover it complex to acquire oil at a lower cost for cost-effective production. The oil is the potential contributor to the cost (more than 80%) of biodiesel manufacturing [36,51]. Fresh oil obtained from an oilseed manufacturer tends to be the chief quality, most consistent and easily available. However, it also is expected to be a very costly resource of vegetable oil. The biodiesel reaction absorbs 11% methanol (% *w/w*) in the transesterification process. Nonetheless, most manufacturers utilize between 18 and 22% methanol to certify a more complete conversion and make use of all quantity of oil during reaction. Small-scale biodiesel production economics can vary considerably depending on specific manufacturer's selection of oil source, machinery, merchandise and the expense of manpower. However, several fundamental controversies affect all small-scale manufacturers. Thus, Present work will deals with the usage of non-edible castor oil as an oil source for biodiesel preparation, because of non-edibility, the castor oil is cheap and

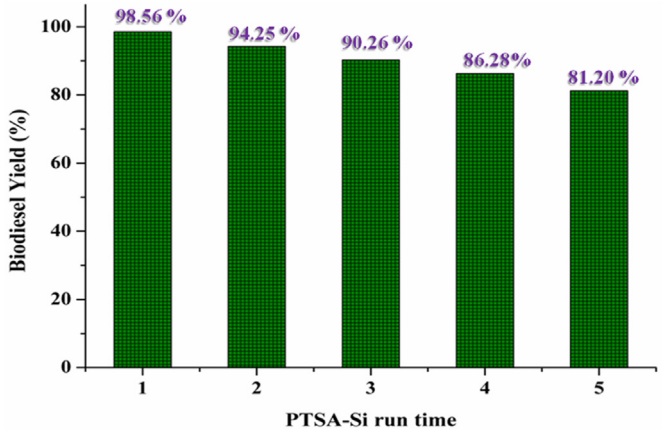

Fig. 12. Impact of PTSA-Si runs time on the (%) yield of biodiesel ((i) 1:11 oil to methanol molar ratio, (ii) 5% PTSA-Si catalyst *(w/w)*, (iii) 65 °C reaction temperature and (iv) 10 h reaction time).

Table 6
Fuel properties of castor biodiesel in contrast to ASTM standards.

Entry No.	Properties	Biodiesel	ASTM Limits	Standard method
1.	Density (40 °C) kg/m^3	872	860–900	EN14214-2008
2.	Flash point (°C)	168	>130	ASTM D92
3.	Kinematic viscosity at 40 °C (mm^2/s)	6.12	1.9-6.0	ASTM D 6751-12
4.	Cetane index	49.85	52.0	ASTM D 976
5.	Cloud point (°C)	−3.4	−15 to 5	ASTM D 2500
6.	Net calorific value (MJ/kg)	40.20	–	IS 1448 P 33 1991
7.	Fire point (°C)	175	>140	ASTM D94
8.	Specific gravity	0.87	0.860–0.900	ASTM D 4052
9.	Acid value (mgKOH/g)	0.64	0.8	ASTM D 6751-09
10	Iodine value (g I_2/100 g oil)	83.24	120	EN14214-2008
11.	Pour point (°C)	−19	−15	ASTM D97
12.	Refractive index	1.45	–	ASTM D 960-79

readily available in the oil market. In addition, reusability of PTSA-Si will be taken in to the account, as heterogeneous class of catalyst. The preparation cost for PTSA-Si would not involve large cost with a view to only single step sulfonation is carried out for its preparation. Therefore, this process would offers an economical biodiesel manufacturing using milder reaction parameters.

4. Conclusion

In current investigation, a promising four time reusable PTSA-Si is freshly prepared and investigated for transesterification of castor oil regarding biodiesel production. It has been manifested against the reaction outcomes; the better relevant reaction parameters for biodiesel synthesis as a means of transesterification of castor oil are; 5% PTSA-Si *(w/w)*, 65 °C reaction temperature, 1:11 O:M molar ratio and 10 h reaction time for 98.56% biodiesel yield. In view of synchronously conduction of an esterification and transesterification by PTSA-Si catalyst, thus, it is not significant to segregate FFAs from castor oil and therefore, it yields economical biodiesel with appreciated conversion.

Declaration of competing interest

The authors declare that they have no known competing financial interests or personal relationships that could have appeared to influence the work reported in this paper.

Acknowledgement

Authors are very much thankful to the S.V. National Institute of Technology, Surat, CSIR, New Delhi, India (Sanction Order Letter No. 02(0170)/13/EMR-II) and Atmiya University, Rajkot (Sanction Order Letter No. SL/SMFAP/Phase 2/2022/004) for financial compensation. We are extremely thankful to the Mechanical Engineering Department, SVNIT, Surat, Department of Chemistry, IIT Madras and Prof. Anamik Shah, Center of Excellence in Drug Discovery, Saurastra University, Rajkot, Gujarat, India for analytical instrumentation facility.

Appendix A. Supplementary data

Supplementary data to this article can be found online at https://doi.org/10.1016/j.cinorg.2023.100005.

References

[1] N. Izadyar, Resource assessment of the renewable energy potential for a remote area: a review, Renew. Sustain. Energy Rev. 62 (2016) 908–923.
[2] J.A. Melero, J. Iglesias, G. Morales, Heterogeneous acid catalysts for biodiesel production: current status and future challenges, Green Chem. 11 (2009) 1285–1308.
[3] P.M. Schenk, Second generation biofuels: high-efficiency microalgae for biodiesel production, Bioenergy Res 1 (2008) 20–43.
[4] I.B. Bankovic-Ilic, O.S. Stamenkovic, V.B. Veljkovic, Biodiesel production from non-edible plant oils, Renew. Sustain. Energy Rev. 16 (2012) 3621–3647.
[5] C.Y. Chen, K.L. Yeh, R. Aisyah, D.J. Lee, J.S. Chang, Cultivation, photobioreactor design and harvesting of microalgae for biodiesel production: a critical review, Bioresour. Technol. 102 (2011) 71–81.
[6] M.M. Gui, K.T. Lee, S. Bhatia, Feasibility of edible oil vs. non-edible oil vs. Waste edible oil as biodiesel feedstock, Energy 33 (2008) 1646–1653.
[7] M. Balat, Potential alternatives to edible oils for biodiesel production-a review of current work, Energy Convers. Manag. 52 (2011) 1479–1492.
[8] H. Ong, Production and comparative fuel properties of biodiesel from non- edible oils: jatropha curcas, sterculia foetida and ceiba pentandra, Energy Convers. Manag. 73 (2013) 245–255.
[9] D. Rajagopal, Rethinking current strategies for biofuel production in India, in: International Conference on Linkages in Water and Energy in Developing Countries Organized by IWMI and FAO, ICRISAT, Hyderabad, India, 2007, pp. 29–30. January.
[10] R. Sattanathan, Production of biodiesel from castor oil with its performance and emission test, Int. J. Sci. Res. 4 (2015) 273–279.
[11] P. Sreenivas, R.M. Venkata, K. Chandra Sekhar, Development of biodiesel from castor oil, Int. J. Energy Sci. 3 (2011) 192–197.
[12] A. Demirbas, Economic and environmental impacts of biofuels: a review, Appl. Energy 86 (2009) 108–117.
[13] A. Demirbas, Importance of biodiesel as transportation fuel, Energy Pol. 35 (2007) 4661–4670.
[14] D.Y.C. Leung, Y. Guo, Transesterification of neat and used frying oil: optimization for biodiesel production, Fuel Process. Technol. 87 (2006) 883–890.
[15] M. Di Serio, M. Cozzolino, M. Giordano, R. Tesser, P. Patrono, E. Santacesaria, From homogeneous to heterogeneous catalysts in biodiesel production, Ind. Eng. Chem. Res. 46 (2007) 6379–6384.
[16] A. Kamal, G. Chouhan, Investigations towards the chemoselective thioacetaliztion of carbonyl compounds by using ionic liquid [bmim]Br as a recyclable catalytic medium, Adv. Synth. Catal. 346 (2004) 579–582.
[17] J.S. Yadav, B.V.S. Reddy, G. Kondaji, Eco-friendly and highly chemoselective 1,3-oxathio- and 1,3-dithioacetalization of aldehydes using ionic liquids, Chem. Lett. 32 (2003) 672–673.
[18] S.H. Xuan, S.F. Lee, J.T.F. Lau, X.M. Zhu, Y.X. Wang, F. Wang, Photocytotoxicity and magnetic relaxivity responses of dual-porous gamma-Fe_2O_3 @meso-SiO_2 microspheres, ACS Appl. Mater. Interfaces 4 (2012) 2033–2040.
[19] I.A.L. Bassan, D.R. Nascimento, R.A.S. Gil, M.I.P. da Silva, C.R. Moreira, W.A. Gonzalez, A.C. Faro Jr., T. Onfroy, E.R. Lachter, Esterification of fatty acids with alcohols over niobium phosphate, Fuel Process. Technol. 106 (2013) 619–624.
[20] E. Lotero, Y. Liu, D.E. Lopes, K. Suwannakarn, D.A. Bruce, J.G. Goodwin, Synthesis of biodiesel via acid catalysis, Ind. Eng. Chem. Res. 44 (2005) 5353–5363.
[21] K. Narasimharao, D.R. Brown, A.F. Lee, A.D. Newman, P.F. Siril, S.J. Tavener, K. Wilson, Structure-activity relations in Cs-doped heteropolyacid catalysts for biodiesel production, J. Catal. 248 (2007) 226–234.
[22] L. Pesaresi, D.R. Brown, A.F. Lee, J.M. Montero, H. Williams, K. Wilson, Cs-doped $H_4SiW_{12}O_{40}$ catalysts for biodiesel applications, Appl. Catal., A 360 (2009) 50–58.
[23] J. Dhainaut, J.P. Dacquin, A.F. Lee, K. Wilson, Hierarchical macroporous-mesoporous SBA-15 sulfonic acid catalysts for biodiesel synthesis, Green Chem. 12 (2010) 296–303.
[24] C. Pirez, A.F. Lee, J.C. Manayil, C.M.A. Parlettb, K. Wilson, Hydrothermal saline promoted grafting: a route to sulfonic acid SBA-15 silica with ultra-high acid site loading for biodiesel synthesis, Green Chem. 16 (2014) 4506–4509.

[25] X. Mo, E. Lotero, C. Lu, Y. Liu, J.G. Goodwin, A novel sulfonated carbon composite solid acid catalyst for biodiesel synthesis, Catal. Lett. 123 (2008) 1–6.
[26] R. Purova, K. Narasimharaoa, N.S.I. Ahmeda, S. Al-Thabaiti, A. Al-Shehri, M. Mokhtar, W. Schwieger, Pillared HMCM-36 zeolite catalyst for biodiesel production by esterification of palmitic acid, J. Mol. Catal. Chem. 406 (2015) 159–167.
[27] A. Corma, From microporous to mesoporous molecular sieve materials and their use in catalysis, Chem. Rev. 97 (1997) 2373–2420.
[28] Q. Shu, Z. Nawaz, J. Gao, Y. Liao, Q. Zhang, D. Wang, Synthesis of biodiesel from a model waste oil feedstock using a carbon-based solid acid catalyst: reaction and separation, Bioresour. Technol. 101 (2010) 5374–5384.
[29] M.A. Olutoye, B.H. Hameed, A highly active clay-based catalyst for the synthesis of fatty acid methyl ester from waste cooking palm oil, Appl. Catal., A 450 (2013) 57–62.
[30] J.A. Melero, L.F. Bautista, J. Iglesias, G. Morales, R. Sánchez-Vázquez, Zr-SBA-15 acid catalyst: optimization of the synthesis and reaction conditions for biodiesel production from low-grade oils and fats, Catal. Today 195 (2012) 44–53.
[31] M.K. Lam, K.T. Lee, A.R. Mohamed, Sulfated tin oxide as solid superacid catalyst for transesterification of waste cooking oil: an optimization study, Appl. Catal. B Environ. 93 (2009) 134–139.
[32] M.R. Monteiro, A.R.P. Ambrozin, L.M. Liao, A.G. Ferreira, Determination of biodiesel blend levels in different diesel samples by ^{1}H NMR, Fuel 88 (2009) 691–696.
[33] Y.K. Yurev, Preparation of *p*-toluene sulfonic acid, Practical work in organic chemistry 1 (1964) 138–139.
[34] M. Vafaeejadeh, A. Fattahi, Calculating the acidity of silica supported alkyl sulfonic acids considering the matrix effect: a DFT study, Phosphorous sulfur and silicon 189 (2014) 849–857.
[35] P. Garcia Moreno, M. Khanum, A. Guadix, E.M. Guadix, Optimization of biodiesel production from waste fish oil, Renew. Energy 68 (2014) 618–624.
[36] B.Z. Dholakiya, Super phosphoric acid catalyzed biodiesel production from low cost feedstock, Arch. Appl. Sci. Res. 4 (2012) 551–561.
[37] H. Muthu, V. Sathya Selvabala, T.K. Varathachary, D. Kirupha Selvaraj, J. Nandagopal, S. Subramanian, Synthesis of biodiesel from neem oil using sulfated zirconia via transesterification, Braz. J. Chem. Eng. 27 (2010) 601–608.
[38] M.A. Ferreira e Santos, I. Pinheiro Lobo, R. Serpa da Cruz, Synthesis and characterization of novel ZrO_2-SiO_2 mixed oxides, Mater. Res. 17 (2014) 700–707.
[39] S. Brunauer, P.H. Emmett, E. Teller, Adsorption of gases in multimolecular layers, J. Am. Chem. Soc. 60 (1938) 309–315.
[40] G. Baskar, S. Soumiya, Production of biodiesel from castor oil using iron (II) doped zinc oxide Nano catalyst, Renew. Energy 98 (2016) 101–107.
[41] N.A. Negm, G.H. Sayed, F.Z. Yehia, O. Habib, E.A. Mohamed, Biodiesel production from one-step heterogeneous catalyzed process of Castor oil and Jatropha oil using novel sulphonated phenyl silane montmorillonite catalyst, J. Mol. Liq. 234 (2017) 157–163.
[42] N.A. Negm, G.H. Sayed, O. Habib, F.Z. Yehia, E.A. Mohamed, Heterogeneous catalytic transformation of vegetable oils into biodiesel in one-step reaction using super acidic sulfonated modified mica catalyst, J. Mol. Liq. 237 (2017) 38–45.
[43] A. Drelinkiewicz, Z. Kalemba-Jaje, E. Lalik, A. Zieba, D. Mucha, E.N. Konyushenko, J. Stejskal, Transesterification of triacetin and Castor oil with methanol catalyzed by supported polyaniline-sulfate. A role of polymer morphology, Appl. Catal., A 455 (2013) 92–106.
[44] T.M. Serra, D.R. de Mendonça, J.P.V. da Silva, M.R. Meneghetti, S.M. Plentz Meneghetti, Comparison of soybean oil and castor oil methanolysis in the presence of tin (IV) complexes, Fuel 90 (2011) 2203–2206.
[45] A. Goswami, Chapter 18, an Alternative Eco-Friendly Avenue for castor Oil Biodiesel: Use of Solid Supported Acidic Salt Catalyst, Chemical Science Block, CSIR- North-East Institute of Science & Technology, Assam, India, 380-396.
[46] R.M. deAlmeida, L.K. Noda, N.S. Goncalves, S.M.P. Meneghetti, M.R. Meneghetti, Transesterification reaction of vegetable oils, using superacid sulfated TiO2–base catalysts, Appl. Catal., A 347 (2008) 100–105.
[47] M. Rengasamy, K. Anbalagan, S. Kodhaiyolii, V. Pugalenthi, Castor leaf mediated synthesis of iron nanoparticles for evaluating catalytic effects in transesterification of castor oil, RSC Adv. 6 (2016) 9261–9269.
[48] H. Yuan, B.L. Yang, G.L. Zhu, Synthesis of biodiesel using microwave absorption catalysts, Energy Fuel. 23 (2009) 548–552.
[49] R. Liu, X. Wang, X. Zhao, P. Feng, Sulfonated ordered mesoporous carbon for catalytic preparation of biodiesel, Carbon 46 (2008) 1664–1669.
[50] H.Y. Shrirame, N.L. Panwar, B.R. Bamniya, Biodiesel from castor oil- A green energy option, Low Carbon Econ. 2 (2011) 1–6.
[51] M.L. Savaliya, B.Z. Dholakiya, A Simpler and highly efficient protocol for the preparation of biodiesel from soap stock oil using BBSA catalyst, RSC Adv. 5 (2015) 74416–74424.

Abbreviations

JCPDS: Joint committee on powder diffraction standards
OMC–SO_3H–: Ordered mesoporous carbon- Sulfonic acid
PAHs: Polycyclic aromatic hydrocarbons
HC: Hydrocarbons
PTSA-Si: p-toluene sulfonic acid-silica
NMR: Nuclear magnetic resonance
FFAs –: Free fatty acids
SEM: Scanning electron microscope
XRD: X-ray diffraction
TGA: DTA-Thermogravimentric analysis- Differential thermal analysis
FT-IR: Fourier transformed infrared spectroscopy
ASTM: American society for testing and materials
AOCS: American oil chemical society
IS: Indian standards
EN: European standards
BET: Brunauer - Emmett – Teller
GC-FID: Gas chromatography- Flame ionization detector
JIS: Japanese industrial standards
BS: British standards
CO: Castor oil
CB: Castor biodiesel